

PAPER REF: To be completed by the Editors

EXPERIMENTAL INVESTIGATION OF LENGTH INFLUENCE ON REMOVABLE LINKS

Adriana Chesoa^{1(*)}, Aurel Stratan¹, Calin Neagu¹, Dan Dubina^{1,2}

¹Department of Steel Structures and Structural Mechanics, Politehnica University Timisoara, Timisoara, Romania

²Fundamental and Advanced Technical Research Centre (CCTFA), Romanian Academy, Timisoara, Romania

(*)Email: adriana.chesoa@upt.ro

ABSTRACT

High seismic hazard zones are found all over the world, arising concerns about life and economic loss in the event of a major earthquake. Thus, structural engineers must find ways to increase seismic safety without attracting excessive costs. One method is to develop efficient structural systems which provide a convenient balance between stiffness and ductility. Eccentrically braced frames (EBFs) are such systems, enabling the reduction of seismic design forces based on a high energy dissipation capacity through the inelastic deformations of beam segments called links. Another method is to reduce the repair costs and downtime of a structure hit by an earthquake. This can be done by implementing the concepts of removable dissipative members (bolted links are intended to provide the energy dissipation capacity and to be easily replaceable) and re-centring capability (provided by the more flexible moment resisting frames) in a dual structure, obtained by combining steel eccentrically braced frames with removable bolted links with moment resisting frames (MRFs). The herein described experimental investigation aims at observing the influence of link lengths (and different bolted connections) on the behaviour and response of such elements, with implications on the re-centering capability of dual EBFs.

Keywords: short bolted links, flush end-plate bolted connection, extended end-plate bolted connection, eccentrically braced steel frames

INTRODUCTION

The seismic performance, re-centring capability and link replacement feasibility of a dual re-centring EBF with removable flush end-plate bolted links have already been experimentally validated within the DUAREM project [1]. In this case, very short links were used in order to achieve the flush end-plate connection overstrength, so it can be kept elastic in order to be able to remove the link. Re-centring capability of EBFs with other types of removable links has not been yet approached. One of the main objectives of an ongoing research project, is to extend experimentally the assessment of cyclic seismic performance and the link replacement feasibility, on extended end-plate bolted links. Links with this type of connection configuration were also previously investigated [2] by others. This type of connection geometry is more rigid than the flush end-plate one and provides a larger connection capacity, thus longer links can be used. Therefore, the first task of the present experimental investigation consists of testing isolated short links assemblies in two solutions (see Fig. 1): flush end-plate bolted link LF (with length $e=500\text{mm} \approx 0.8 M_{p,link}/V_{p,link}$) and extended end-plate bolted link LE (with length $e=1000\text{mm} \approx 1.6 M_{p,link}/V_{p,link}$), at natural scale. $V_{p,link}$ and $M_{p,link}$ represent the shear force and bending moment design resistances of an I section seismic link, as defined by EN1998. For

each of the mentioned assemblies, two tests are performed: one monotonic (m) and one cyclic (c), in order to obtain the response in terms of stiffness, capacity, overstrength and ductility.

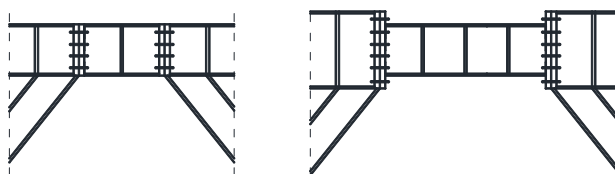


Fig. 1 – Flush (F) and extended (E) end-plate bolted links

TEST SETUP

The experimental setup for testing isolated links assemblies is illustrated in Fig. 2. The force generated by a 1500 kN hydraulic actuator was applied to links assemblies by means of a frame (2.75 meters height and 2.2-2.5 meters width) consisting of two HEB340 columns pinned at the base and one IPE360 pinned member, generating shearing of the test specimen.

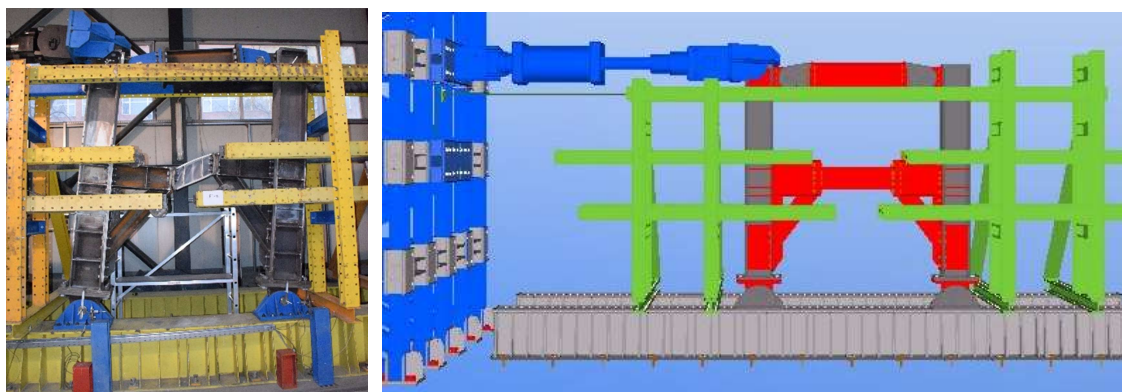


Fig. 2 – Experimental setup for testing isolated links assemblies

The prototype structures [3] from which the test specimens (see Table 1) were extracted, were designed according to EN1990, EN1991, EN1992, EN1993, EN1994 and EN1998. Gravity loads of 5 kN/m² (permanent load) and 3.8 kN/m² (live load) were considered. The structures were assumed to be located in an area characterised by 0.3g peak ground acceleration and stiff soil conditions (EC8 spectrum for soil type C). A behaviour factor $q = 4$ and inter-storey drift limitation of 0.0075 of the storey height were assumed. The structural steel components were designed using S355 grade steel.

Table 1 – Test specimens description

Specimen	Pieces	Length e	Physical length [mm]	Welded I section (h x b x tf x tw)	Bolted connection
LF	2	$\approx 0.8 M_{p,link} / V_{p,link}$	500	250 x 150 x 15 x 6	Flush end-plate
LE	2	$\approx 1.6 M_{p,link} / V_{p,link}$	1000	250 x 150 x 15 x 6	Extended end-plate

The instrumentation of the experimental mock-up consisted of 10 local displacement transducers (see Fig. 3): DT1 and DT2 to monitor the total link deformations, D1 and D2 to monitor only web panel deformations, DC1 to DC4 to monitor connections' rotations and DS1 and DS2 to monitor slips in connections; and 6 global displacement transducers to monitor the global displacements of the setup: horizontal and vertical slips in both columns' bottom pins, lateral top displacement of the setup and relative horizontal top displacement between the two

columns. Potential dissipative areas (links – especially their webs) were white-washed to visually observe yielding.

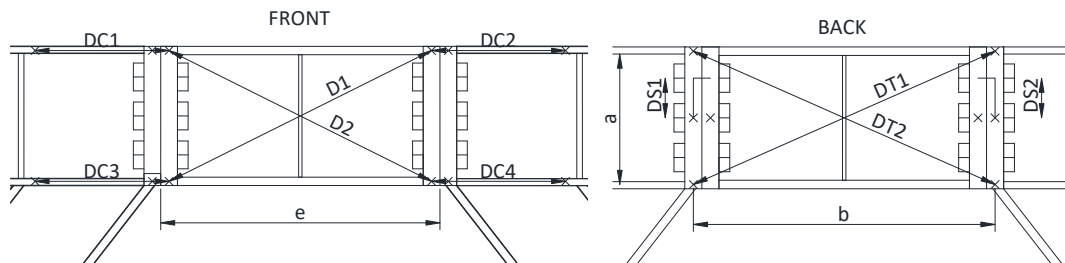


Fig. 3 – Link local displacement transducers layout

EXPERIMENTAL PROGRAMME

Two experimental displacement controlled tests were performed, on each specimen type (see Table 2): one monotonic, followed by a cyclic test using the AISC [4] loading protocol for links (see Fig. 4).

Table 2 – Experimental sequence

Test	Type	Specimen
LF1-M	monotonic	LF1
LF2-C	cyclic	LF2
LE1-M	monotonic	LE1
LE2-C	cyclic	LE2

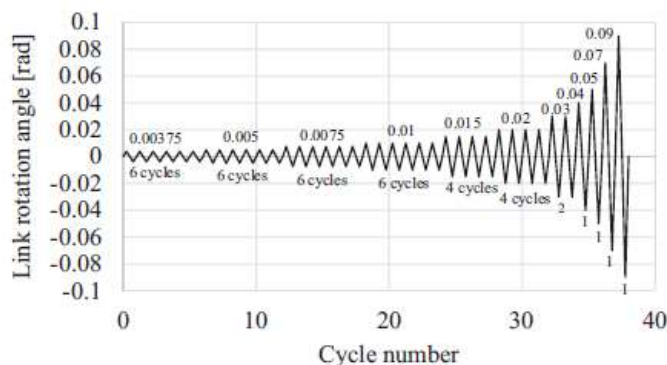


Fig. 4 - AISC loading protocol for links

After each test, the damaged shear link is unbolted and replaced with the following new link. The rest of the test setup is being used for all the four tests, remaining elastic during the process. Just the beams from the flush end-plate configuration were replaced when testing the extended end-plate one, and the right column was re-positioned to the right to fit the longer extended end-plate specimen.

EXPERIMENTAL RESULTS

The response of the experimental specimens is characterized by the relationship between link shear force and link shear rotation. The shear force in links (V) was obtained using the actuator force (FA) and the geometry of the experimental setup, according to Fig. 5 and the following formula:

$$V = FA * \frac{H}{L}$$

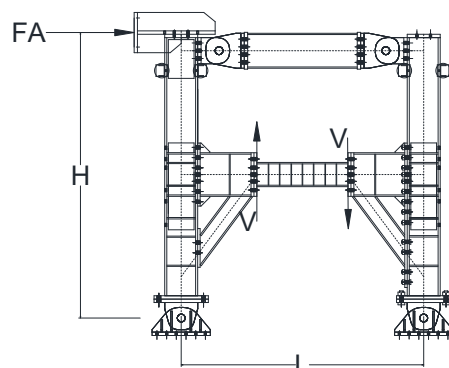


Fig. 5 – Experimental setup geometry

The link shear rotation (γ_T) was obtained from the displacement transducers that recorded the total link deformations (DT1 and DT2), according to Fig. 3 and the following formula, related to length e :

$$\gamma_T = \frac{2 * \sqrt{a^2 + b^2} * (DT2 - DT1) + (DT2^2 - DT1^2)}{4 * a * b} * \frac{b}{e}$$

The initial stiffness K_{ini} was determined by the linear relation between 50 kN and 150 kN shear force. The yield shear force V_y was established at a reduction of the tangent stiffness of 15% from the initial one. The ultimate deformation γ_{Tu} was established at a shear force reduction under 80% of the yield shear force.

The M30 10.9 bolts in each connection were pre-tensioned according to the combined method [5], applying a torque of 1150 kNmm (75%) using a hydraulic wrench and an additional rotation of 90 degrees, in case of LF specimens and at 75% in case of LE specimens.

LF1-M test

The first test of the experimental sequence was the displacement controlled monotonic one, using the first flush end-plate shear link LF1, applying displacement until the shear failure of the specimen, represented by the failure of link web and flange by cracking in the weld heat-affected zone, followed by failure of bolts from the first bolt row in tension in one connection (see Fig. 6), the rest of the setup remaining elastic.



Fig. 6 – Failure mode of the end of LF1-M specimen

The damaged link was then removed by unscrewing bolts and even flame cutting those from the first bolt row in tension in the other connection, which were too deformed for simply unscrewing.

The experimental shear force - shear deformation relationship for LF1-M test is illustrated in Fig. 7, showing also the initial stiffness K_{ini} , the yield shear force V_y , the maximum shear force V_{max} and the ultimate shear deformation γ_{Tu} .

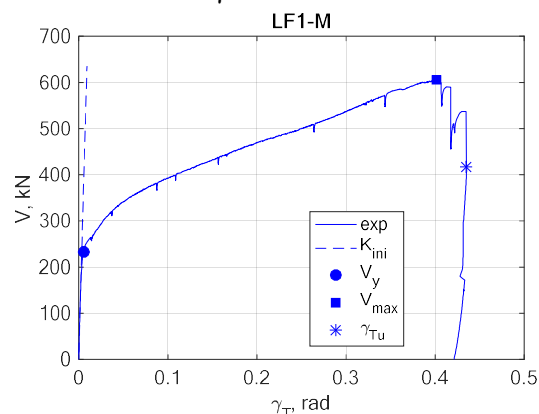


Fig. 7 – Experimental shear force – shear deformation relationship for LF1-M specimen

LF2-C test

The second test of the experimental sequence was the displacement controlled cyclic one, using the second flush end-plate shear link LF2 and applying the AISC loading protocol (monitoring the shear link rotation) until the shear cyclic failure of the specimen, represented by the failure of link web by cracking in the weld heat-affected zone (see Fig. 8), the rest of the setup remaining elastic.



Fig. 8 –Failure mode of the LF2-C specimen

The damaged link was then removed by unscrewing all the bolts.

The experimental shear force - shear deformation relationship for LF2-C test is illustrated in Fig. 9. The positive and negative envelopes of this cyclic test are illustrated in Fig. 10, showing also the initial stiffness K_{ini} , the yield shear force V_y , the maximum shear force V_{max} and the ultimate shear deformation γ_{Tu} , for each of them.

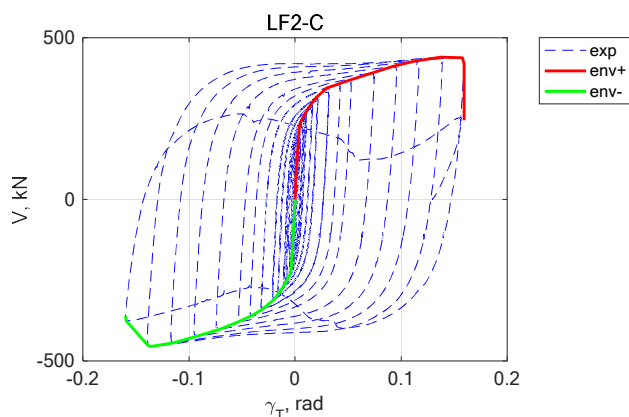


Fig. 9 - Experimental shear force – shear deformation relationship for LF2-C test

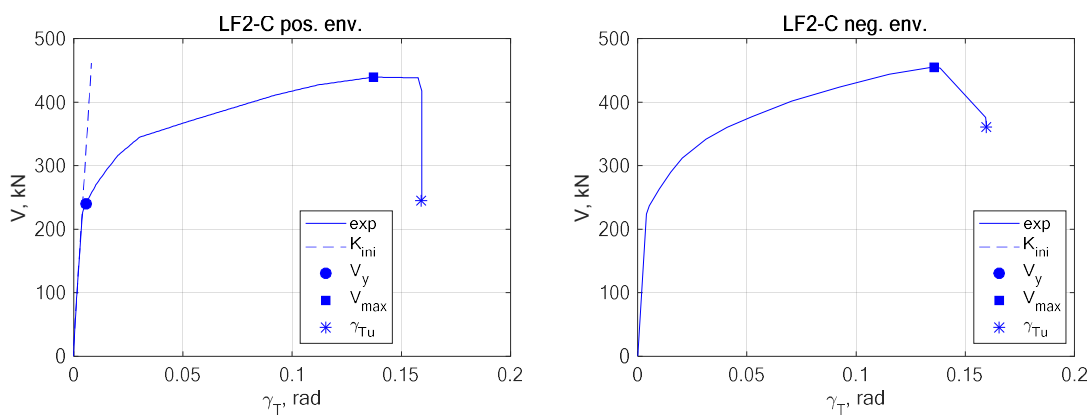


Fig. 10 – Positive and negative envelopes of the LF2-C specimen

LE1-M test

For the following two tests, the beams were replaced with the larger sections for the extended end-plate configuration, and the right column of the setup was re-positioned 300 mm to the right to fit the longer specimen.

The third test of the experimental sequence was the displacement controlled monotonic one, using the first extended end-plate shear link LE1, applying displacement until the shear failure of the specimen, represented by the failure of link flanges in the tensioned parts and propagation of cracks in the web, in the weld heat-affected zone) (see Fig. 11), the rest of the setup remaining elastic.



Fig. 11 – LE1 link deformation and failure at the end of LE1-M test

The damaged link was then removed by unscrewing all the bolts. The experimental shear force - shear deformation relationship for LE1-M test is illustrated in Fig. 12, showing also the initial stiffness K_{ini} , the yield shear force V_y , the maximum shear force V_{max} and the ultimate shear deformation γ_{Tu} .

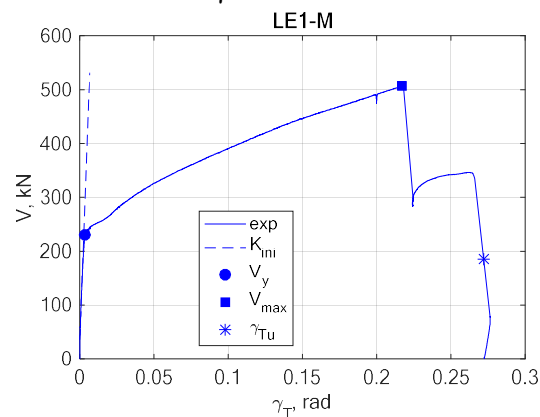


Fig. 12 - Experimental shear force – shear deformation relationship for LE1-M test

LE2-C test

The fourth test of the experimental sequence was the displacement controlled cyclic one, using the second extended end-plate shear link LE2, applying the AISC loading protocol (monitoring the shear link rotation) until the shear cyclic failure of the specimen, represented by the failure of link flanges and propagation of cracks in the web, in the weld heat-affected zone (see Fig. 13), the rest of the setup remaining elastic.

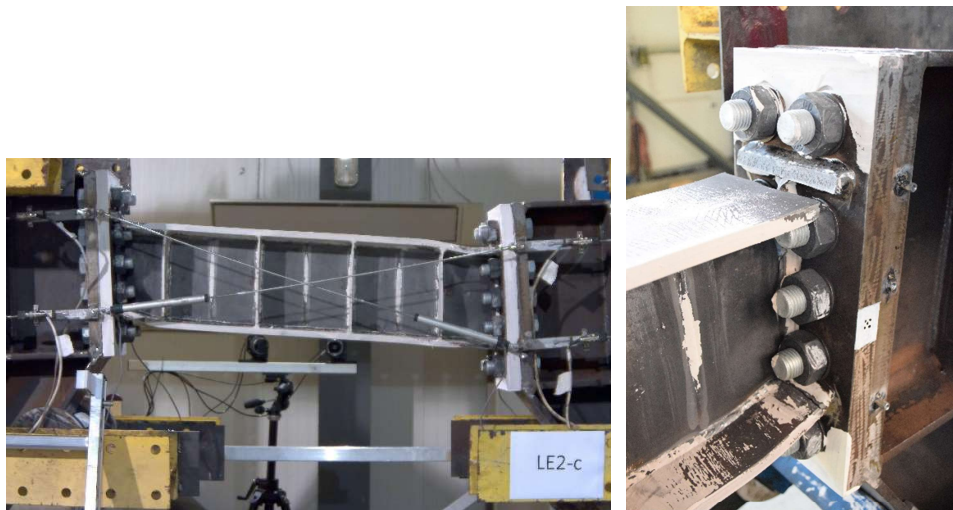


Fig. 13 – LE2 link deformation and failure at the end of LE2-C test

The damaged link was then removed by unscrewing all the bolts. The experimental shear force - shear deformation relationship for LE2-C test is illustrated in Fig. 14. The positive and negative envelopes of this cyclic test are illustrated in Fig. 15, showing also the initial stiffness K_{ini} , the yield shear force V_y , the maximum shear force V_{max} and the ultimate shear deformation γ_{Tu} , for each of them.

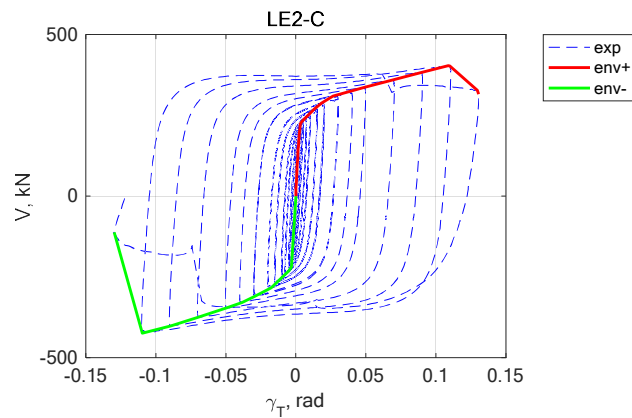


Fig. 14 - Experimental shear force – shear deformation relationship for LE2-C test

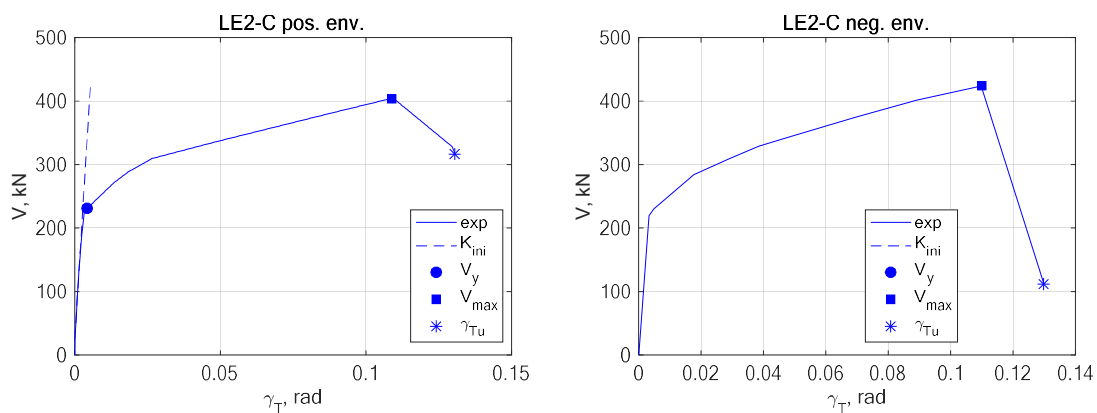


Fig. 15 – Positive and negative envelopes of the LE2-C cyclic test

Results comparison

The initial stiffness K_{ini} , the yield shear force V_y , the maximum shear force V_{max} (both positive and negative for cyclic tests), the overstrength V_{max} / V_y (both positive and negative for cyclic tests) and the ultimate shear deformation γ_{Tu} (both positive and negative for cyclic tests), for all four experimental specimens are presented in Table 3 and Fig. 16 and Fig. 17.

Table 3 – Experimental tests results

Test	K_{ini} [kN/rad]	V_y [kN]	V_{max} -pos. [kN]	V_{max} -neg. [kN]	V_{max} / V_y pos.	V_{max} / V_y neg.	γ_{Tu} -pos. [rad]	γ_{Tu} -neg. [rad]
LF1-M	68174	233.9	605.0	-	2.59	-	0.435	-
LF2-C	54423	239.6	439.5	455.5	1.83	1.90	0.159	0.159
LE1-M	73608	231.1	506.2	-	2.19	-	0.272	-
LE2-C	73990	230.8	404.2	423.8	1.75	1.84	0.131	0.130

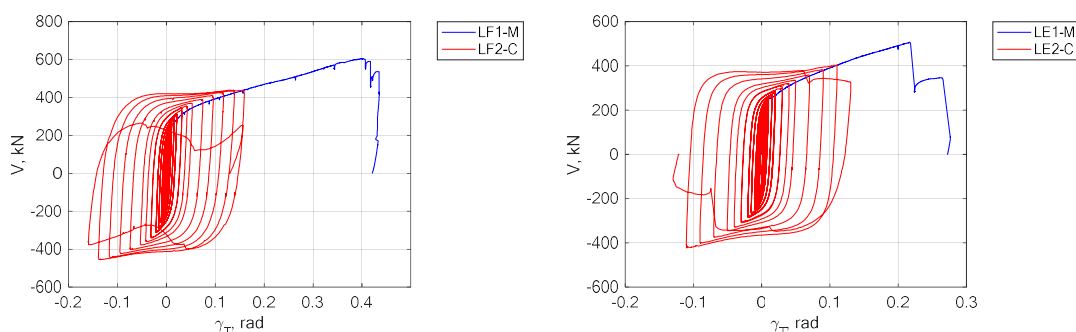


Fig. 16 – Comparison between monotonic and cyclic tests, for both LF and LE links

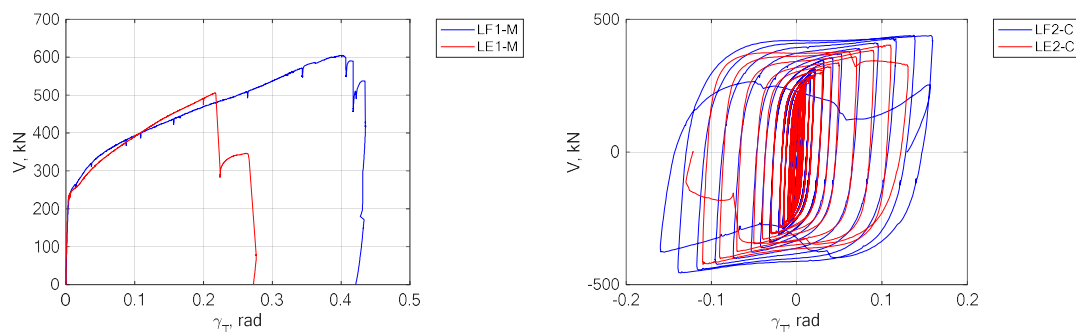


Fig. 17 – Comparison between LF and LE links behaviour, both monotonic and cyclic

The elastic response of the tested specimens is described by their initial stiffness K_{ini} . A decrease in initial stiffness is observed in case of the cyclic test of LF specimen with regard to the monotonic one (roughly 20%) and this may be due to a difference in actual bolt pre-tensioning and/or mounting gaps between end plates (filled with additional 1-2 mm thin plates).

The inelastic response of the tested specimens is described by the following parameters.

Yield shear force V_y is similar for all four specimens (less than 5% difference), all shear links having the same cross-section. We can observe maximum shear forces smaller within the cyclic tests, with respect to the monotonic ones: about 27% for LF specimen and 20% for LE specimen, simply because deformations from monotonic tests have just not been reached within the cyclic ones.

The investigated shear links overstrength proved to be larger than the one estimated pre-test, especially for the LE specimen: 1.83 (1.90 negative) for the LF specimen (very close to the pre-test estimation of 1.80, at least for the positive branch) and 1.75 (1.84 negative) for the LE specimen (pre-test estimated at 1.50).

During the cyclic tests, the LF specimen proved to be with 20% more ductile than the LE one: the ultimate shear deformation being 0.159 rad for the LF specimen and 0.131 rad for the LE specimen, compared to the capacity of shear links stated by ASCE 41-13 [6] of 0.15 rad. In case of monotonic tests, LF specimen proved to be significantly more ductile than the LE one, with 60%.

But the absolute values of the ultimate shear deformations (in mm), for the LE specimen are significantly larger (65%) than for the LF specimen (131 mm compared to 79.5 mm).

CONCLUSIONS

When using flush end-plate connections for the bolted links, very short lengths ($e \leq 0.8 M_{p,link} / V_{p,link}$) are necessary in order to provide the connection capacity within the given geometry. This leads to larger links overstrength. By adopting extended end-plate connections, shear links could also be designed longer ($e \leq 1.6 M_{p,link} / V_{p,link}$), providing the connection capacity within the given geometry. In case of the present experimental investigation, this leads to just slightly smaller links overstrength (about 5%), for this type of configuration.

During the cyclic tests, and even more obviously during the monotonic ones, it was observed that crack evolution is different from one specimen to another: in case of LF links, cracks were firstly and predominantly observed in the link's web, and only at large deformations, they appear also in link's flanges, while in case of LE links, the order is inverse. This can be rationally explained by the larger influence of bending moment on LE specimens, that are still shear links (at the limit with intermediate ones, as defined by EC8), but longer than LF ones.

ACKNOWLEDGMENTS

This work was supported by a grant of Ministry of Research and Innovation (Romania), CNCS - UEFISCDI, project number PN-III-P1-1.1-PD-2016-1655, within PNCDI III.

REFERENCES

- [1]-Ioan A, Stratan A, Dubina D, Poljansek M, Molina F J, Taucer F, Pegon P and Sabau G 2016 Experimental validation of re-centring capability of eccentrically braced frames with removable links Eng Struct 113 p 335-346
- [2]-Mansour N, Christopoulos C and Tremblay R 2011 Experimental validation of replaceable shear links for eccentrically braced steel frames J Struct Eng 137 p 1141-1152.
- [3]- Chesoa A, Stratan A, Dubina D 2019 Influence of link length on re-centring capability of dual eccentrically braced frames, CiBv2019, accepted for publishing in IOP Conference Series: Materials Science and Engineering (MSE) in 2020
- [4]-ANSI/AISC 341-16, Seismic Provisions for Structural Steel Buildings
- [5]-EN 1090-2:2008, Execution of steel structures and aluminium structures, Part 2 – Technical requirements for the execution of steel structures.
- [6]-ASCE/SEI 41-13, Seismic Evaluation and Retrofit of Existing Buildings